Effect of the Crystallization Conditions on the Phase Behavior of Syndiotactic Polystyrene/Poly(phenylene oxide) Blends

G. Dutt, K. M. Kit

Department of Materials Science and Engineering, University of Tennessee, Knoxville, Tennessee 37996-2200

Received 20 August 2001; accepted 3 June 2002

ABSTRACT: Syndiotactic polystyrene (sPS) and poly(phenylene oxide) (PPO) blends, miscible in the melt state, were crystallized from the melt and the quenched state at different temperatures. The effect of the crystallization temperature on the phase behavior of the blends and the polymorphic changes in sPS was investigated by dynamic mechanical analysis (DMA), wide-angle X-ray diffraction (WAXD), and density measurements. In most blends, the crystallization of sPS induced segregation into two homogeneous amorphous phases of different compositions. The temperatures of the DMA relaxations of the neat homopolymers and crystallized blends were fit by the Gordon–Taylor relation to calculate the compositions of these phases. In melt-crystallized blends, with slower crystallization, the major amorphous phase became sPS-rich, whereas the minor phase became PPO-rich. These major and minor amorphous phases could be tentatively assigned to interfibrillar and interlamellar regions, respectively. In cold-crystallized blends, slower crystallization decreased the sPS concentration in both phases, and the scale of segregation was much smaller. WAXD studies and density measurements indicated a complex polymorphic behavior of sPS after it was blended with PPO. © 2003 Wiley Periodicals, Inc. J Appl Polym Sci 87: 1975–1983, 2003

Key words: syndiotactic polystyrene; poly(phenalene oxide); blends; crystallization; phase separation

INTRODUCTION

Syndiotactic polystyrene (sPS) is a stereoregular form of polystyrene that has been shown to be completely melt-miscible with poly(2,6-dimethyl-1,4-phenylene oxide) (PPO)[1] and atactic polystyrene (aPS).[2] It has also been shown that, in these blends, sPS crystallizes to form spherulitic structures.[3,4] In view of the commercial success of aPS/PPO blends, understanding the effect of the crystallizability of sPS on the structure–property relationships in sPS/PPO blends has become important.

As shown for other blends with one crystallizing component,[5–8] it should be possible to control the redistribution of the amorphous component of a miscible sPS/PPO blend through variations in the crystallization conditions (most importantly the crystallization rate, molecular weight, and local composition). In these types of systems, the mobility of the amorphous diluent(s), the crystal growth rate, and the segmental interactions between the components determine the length scale of segregation.[9] Keith and Padden,[10] in their theory of spherulitic crystallization and bundle formation, predicted that the diameter of these bundles should be of the order of a parameter they called the diffusion length (δ). δ is equal to the ratio of the diffusion coefficient (D) of the rejected noncrystallizable species to the crystalline growth rate (V): $\delta = D/V$. D depends on the glass-transition temperature (T_g) of the rejected species (and, therefore, on the composition of the amorphous melt) and the temperature at the growth front. The interactions between the blend components (the interaction parameter χ), the blend composition, and the temperature affect the crystallization rate.

Depending on these factors, amorphous materials of different compositions may be trapped in different proportions between the growing spherulites (interspherulitic segregation), pockets between the lamellar bundles (interfibrillar segregation), and individual lamellae (interlamellar segregation). Several studies have been made with microscopy[11] and mechanical/dielectric spectroscopy techniques combined with small-angle X-ray scattering to determine the actual location of the noncrystallizable species.[12–14]

The effect of the crystallization temperature (T_c) on the phase behavior of the melt-miscible sPS/PPO blends, crystallized from the melt and the quenched state, is reported in this work. The corresponding changes in the compositions of the amorphous phases and the resulting polymorphic changes in the sPS are also discussed. The spherulitic morphologies devel-

Correspondence to: K. M. Kit (kkit@utk.edu).

Contract grant sponsor: DuPont Educational Aid Program.

Journal of Applied Polymer Science, Vol. 87, 1975–1983 (2003)

oped and their relation to the ultimate tensile properties and the mode of spherulitic fracture will be reported in the next article.

EXPERIMENTAL

Materials

The sPS used for this study (Questra LA 320) was kindly provided by Dow Chemical Co. (Midland, MI). The given weight-average molecular weight (M_w) of the resin was 320,000. T_g and the melting point (T_m) were found to be 97.1 and 272.2°C, respectively, through the heating of the as-received polymer in a PerkinElmer DSC 7 (Shelton, CT) at 20°C/min. T_g and T_m for as-received PPO (M_w = 50,000; Scientific Polymer Products, Inc., Ontario, NY) were found to be 219.5 and 268.0°C. The as-received PPO was approximately 5% crystalline, as determined by differential scanning calorimetry (DSC). After blending and molding processes, no indication of PPO melting was observed by DSC. The number-average molecular weights of both polymers were unknown.

Melt blending

sPS and PPO were melt-blended in a twin-blade Brabender mixer measuring head at 290–295°C. Irganox 1076B (0.3% by mass) was used as an antioxidant. The blending was performed for approximately 12 min, after which the formed homogeneous mixture was scraped out and broken down into small pellets in a kitchen blender. Three sPS/PPO compositions (83/17, 67/33, and 50/50) were melt-blended in two batches each. The three different blends were designated sPS83PPO, sPS67PPO, and sPS50PPO, the middle digits denoting the weight percentage of sPS in the blend.

DSC

The thermal analysis of the quenched blends was carried out in a PerkinElmer DSC 7 in a purging nitrogen atmosphere. The blend (6–8 mg) was heated to 305°C, at a rate of 20°C/min and was kept at that temperature for 8 min so that complete melting was ensured. The sample pan was then taken out of the sample chamber and quickly quenched in liquid nitrogen. It was then heated from 25 to 300°C at a rate of 10°C/min. T_g was taken to be the temperature at the center of the transition.

Crystallization

The blend samples for dynamic mechanical analysis (DMA) were crystallized from the melt (melt crystallization) and the quenched state (cold crystallization) into 0.3-mm-thick films in a Wabash hot press (Wabash, IN). Dog-bone-shaped samples for tensile testing were molded in an Atlas mixing molder (Chicago, IL) and then crystallized in the hot press. The hot press was calibrated in an aPS melt with an external thermocouple. First, the powdered blends were put in an aluminum frame and melted in a furnace. The samples to be cold-crystallized were taken out of the furnace, immediately quenched in an ice bath, and then transferred to the preheated hot press. The cold-crystallization temperatures were 180, 190, and 220°C. For melt crystallization, the samples from the furnace were transferred directly to the hot press preheated to T_c. Melt crystallization was performed at 220, 245, and 255°C.

Wide-angle X-ray diffraction (WAXD)

We performed WAXD studies on the quenched, cold- and melt-crystallized blend samples to calculate the crystallinity index and to study the phase changes in sPS after blending. A Rigaku diffractometer (Tokyo, Japan), in the reflection mode, was used with Cu Kα (λ = 1.542 Å) radiation. A silicon standard (2θ = 28.465°) was used to calibrate the instrument. The operating voltage and current of the tube were kept at 35 kV and 30 mA, respectively. The range of the 2θ scan was 5–40°, and the scan step size was 0.03°. The Peak Fit program (Brabender, South Hackensack, NJ) was used to fit Gaussian peaks for reflections from crystalline and amorphous regions by the second derivative method. The weight-fraction crystallinity was then calculated from the ratio of the areas of the crystalline peaks to the total area under the scattering curve from 5–40°. Scattering factor corrections were not made.

DMA

Dynamic mechanical relaxation measurements were made on a Rheovibron viscoelastometer (Toyo Instruments, Tokyo, Japan) operated in the tensile mode. The storage modulus (E') and mechanical loss tangent (tan δ) were obtained at a fixed frequency of 1.1 Hz. A temperature sweep from 70 (or 75) to 250°C was performed at a heating rate of 1°C.

RESULTS AND DISCUSSION

The crystallization times were determined from spherulitic impingement times observed under the polarized optical microscope and from times required for the completion of the isothermal crystallization exotherm in DSC. Melt-crystallized samples were crystallized 50% longer than the time taken for the spherulite impingement. For the quenched blends, a fast primary stage was followed by a slow secondary stage during crystallization. This resulted in a second exotherm in the isothermal crystallization in DSC.

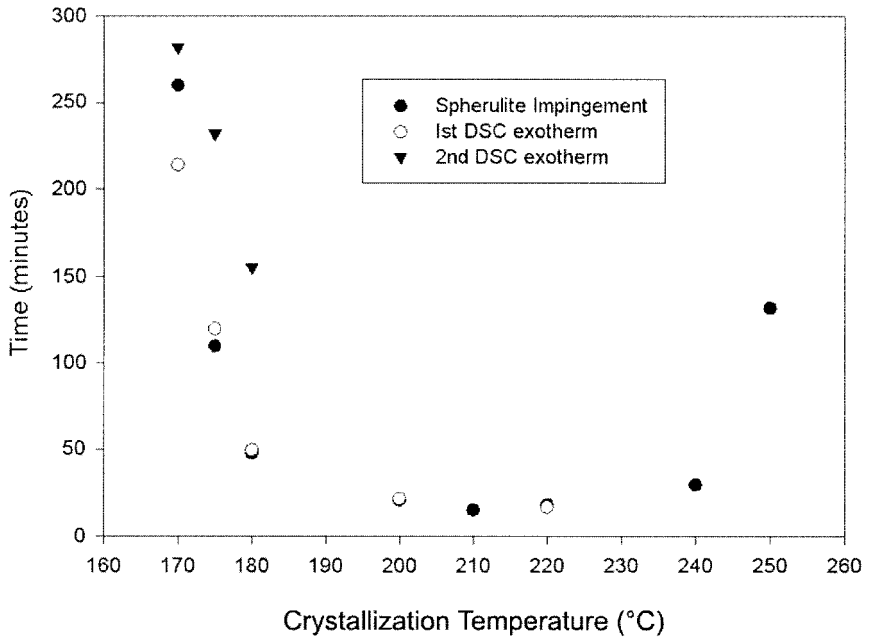

Figure 1 Crystallization times for sPS50PPOs blend by microscopy and DSC.

Therefore, the quenched samples were put for twice the time required for the completion of the second exotherm. The times taken for the spherulite impingement and the DSC exotherms for the crystallized sPS50PPO blend are shown in Figure 1.

DSC

The DSC scans of melt-quenched blends of different compositions and neat homopolymers are shown in Figure 2. A well-defined, composition-dependent glass transition was observed for all the compositions. This clearly suggests that, at all compositions, the blends were miscible to the segmental level in the melt. The pronounced effect of PPO on the crystallization and melting of sPS was also evident. With the increase in the PPO content, the crystallization exotherm during the heating scan became smaller and occurred at higher temperatures and over a wider range of temperatures. Also, T_m of sPS decreased with

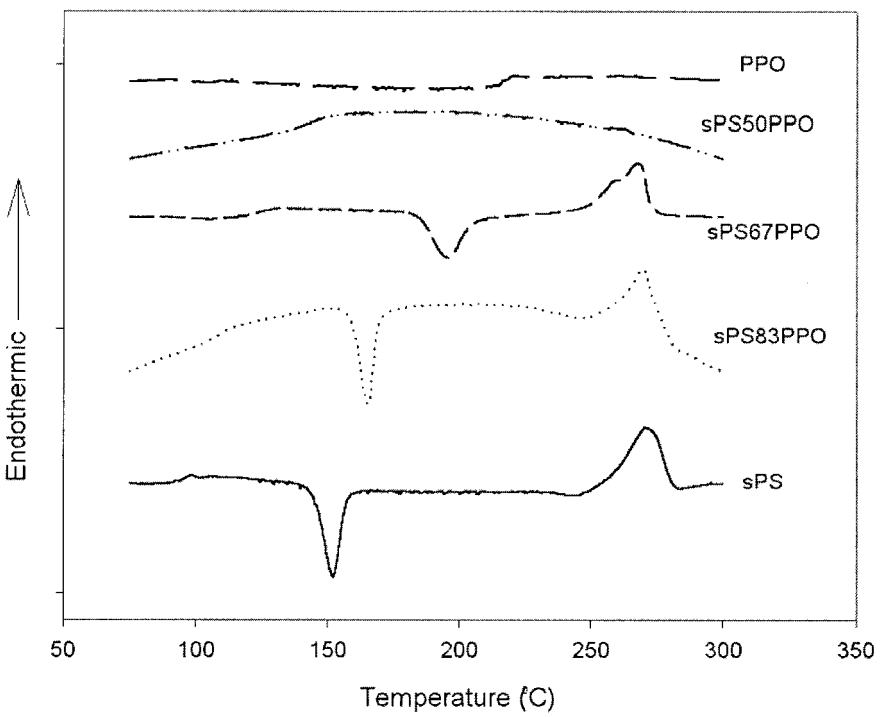

Figure 2 DSC curves for quenched sPS/PPO blends (heating rate = 10°C/min).

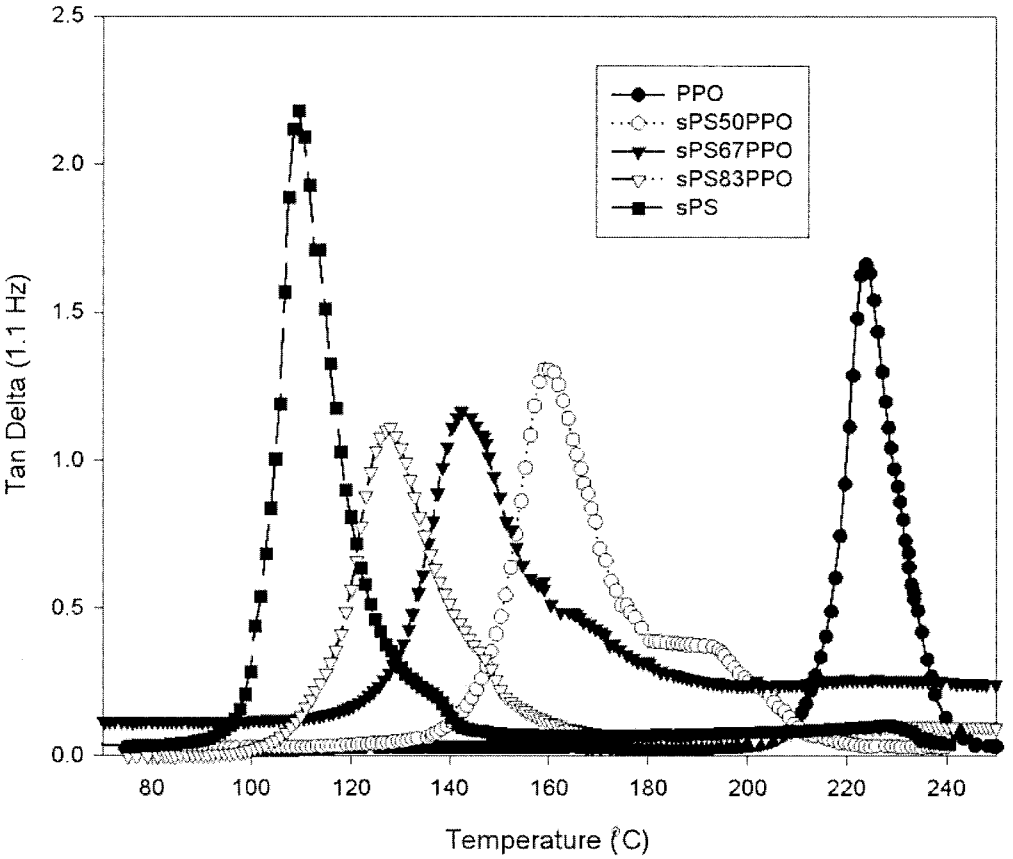

Figure 3 DMA tan δ values of quenched sPS/PPO blends at 1.1 Hz.

increasing PPO content. In the sPS50PPO blend, on heating, the crystallization exotherm could be not seen at all. The increase in T_c and decrease in T_m, with increasing PPO content suggested that PPO strongly interfered with the crystallization of the amorphous sPS. These effects also indicated a segmental-level miscibility. Guerra et al.[1] reported the same trend for quenched sPS/PPO blends. They showed that the behavior of the miscible sPS/aPS blend was completely different; in this system, the T_c values and the degrees of crystallinity of the sPS component remained almost unchanged. As they suggested, the increase in T_c in the sPS/PPO system was due to the large difference in T_g's of sPS and PPO. T_g of the blend increased with the segmental-level mixing of high-T_g PPO.

DMA

Quenched blends

The tan δ values of the quenched sPS/PPO blends from the dynamic mechanical measurements at 1.1 Hz are shown in Figure 3. A composition-dependent relaxation peak can be seen in all the scans. This indicates segmental homogeneity in the amorphous phase. Neat sPS and all the blends showed a long horizontal shoulder to the relaxation peak. This shoulder might be due to either cold crystallization during heating or the relaxation of a second amorphous phase present in the segregated blend. That these shoulders were due to the crystallization of sPS and the reorganization of smaller crystals during the annealing of predominantly amorphous samples from the quenched state was confirmed by the behavior of E' during the heating scan. (The crystallization during heating led to modulus recovery.) The shoulders became broader with increasing PPO content, and this was consistent with slower crystallization at these compositions.

Several T_g–composition analysis relations were used to fit the relaxation temperature (taken as the position of the tan δ maximum) to the composition and the relaxation temperatures of the quenched, neat sPS and PPO. The composition-dependent T_g's predicted by the Kelly–Bueche equation,[15] the Flory–Fox equation,[16] the linear Gordon–Taylor equation,[17] and the Couchman–Karasz relation[18] were compared with the relaxation temperatures obtained from DMA. Details on these T_g–composition analysis relations for miscible blends were presented by Aubin and Prud'homme[19] The Gordon–Taylor equation is as follows:

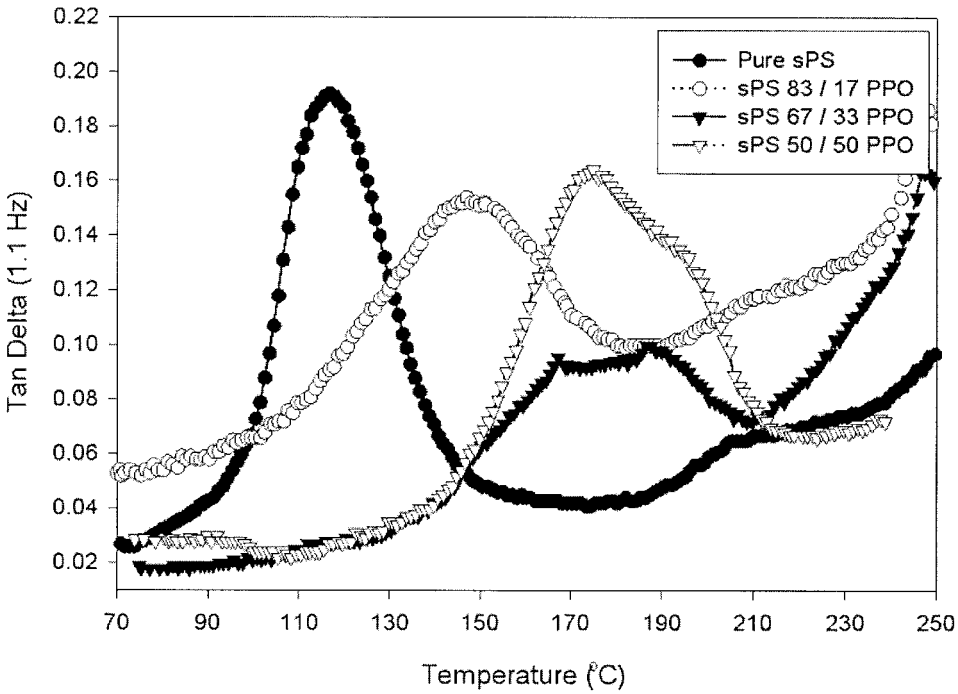

Figure 4 DMA tan δ values of sPS/PPO blends cold-crystallized at 180°C.

$$T_g = \frac{wiT_{g1} + kw_1T_{g1}}{w_1 + kw_2}$$

where w_i and T_{gi} are the weight fraction and glass-transition temperature of the component i, respectively. The parameter k, which is the ratio of the change in the thermal expansion coefficients of the neat polymers between the rubbery and glassy states, was found to be 0.83 for the best fit to the experimental data. This value of k was then used to predict the compositions of the amorphous phases of the crystallized blends and is discussed later.

Cold-crystallized blends

The tan δ values for different sPS/PPO blends cold-crystallized at 180°C are shown in Figure 4. The effect of T_c on the relaxation of the cold-crystallized sPS50PPO blends is shown in Figure 5. In all these DMA scans, the E' recovery shoulders observed in quenched blends were absent. Instead, the scans of the sPS50PPO and sPS67PPO blends, cold-crystallized at different temperatures, showed a distinct shoulder to the major relaxation peak observed in the quenched amorphous blends. For the sPS83PPO blends, the shoulder was very small. Because these shoulders were not accompanied by any modulus recovery in the E' scan, it can be concluded that the shoulders to the primary relaxation peaks indicated segregation of the uniform amorphous phase in the quenched blend into two distinct, but homogeneous, amorphous phases of different compositions. The intensity of the shoulder was much smaller than the primary relaxation, indicating that the relative amount of the second phase was much smaller. No evidence of pure sPS or PPO domains was observed. Greater separation between the main peak and the shoulder for lower T_c values (lower crystallization rates) was likely a result of a greater extent of PPO segregation.

The compositions of the homogeneous amorphous phases present after crystallization from sPS50PPO and sPS67PPO blends were calculated with the maximum positions of fits to the tan δ data and the Gordon Taylor equation ($k = 0.83$). Because the transition temperatures in the crystallized blends were possibly higher on account of the constraining effect of the crystallites on the amorphous domains, these calculated compositions should be treated as a relative indication of the variations in the phase compositions with the change in T_c (Fig. 6). For all cold-crystallized blends, crystallization at 220°C resulted in both amorphous phases with the highest sPS contents. Because among all the temperatures the crystallization rate was highest at this temperature, small, less perfect sPS crystals were formed and overall crystallinity was low. With decreasing temperature (and decreasing crystallization rate), the sPS concentration in both the amorphous phases decreased. The crystallinity index of these cold- and melt-crystallized blends calculated from WAXD spectra on the basis of the actual sPS content is shown in Figure 7. The changes in the slope of the sPS concentration lines between different T_c's can be followed with the crystallinity changes. The higher slope between 180 and 190°C was reflected in

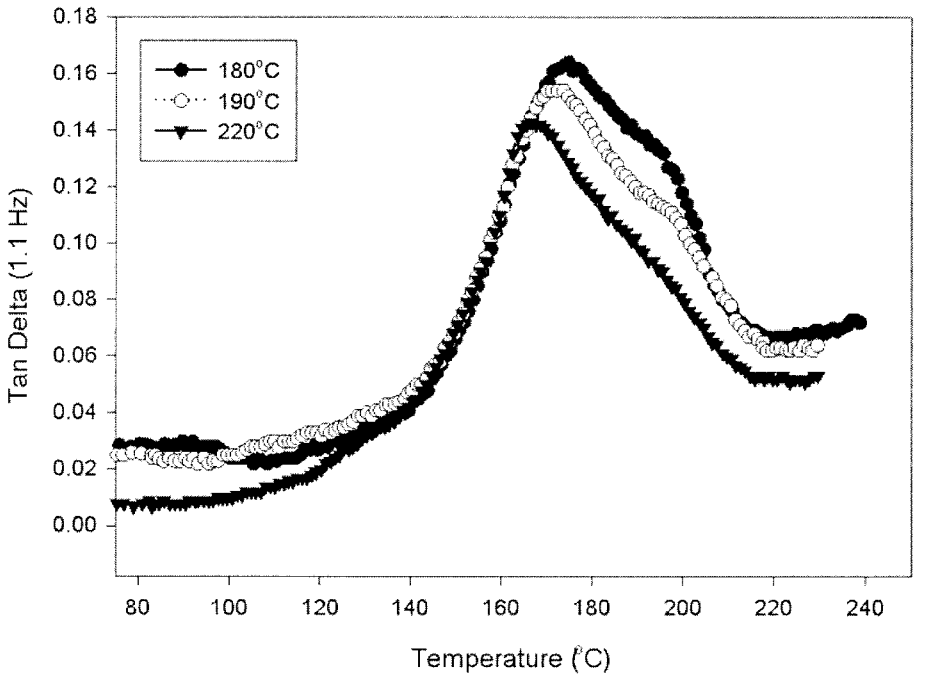

Figure 5 DMA tan δ values of cold-crystallized sPS50PPO blends.

the sharper decrease in the crystallinity (especially for the sPS67PPO blends). As expected, higher crystallinity reduced the sPS amorphous concentration and resulted in amorphous phases richer in PPO.

The identification of these amorphous phases as interspherulitic or interlamellar and intralamellar is difficult. The scanning electron micrographs (reported in the following article) of these quenched sPS/PPO blends cold-crystallized at large supercoolings suggest that a large number of nuclei were formed. These nuclei grew into relatively imperfect spherulites among which it was difficult to distinguish between the interlamellar and intralamellar regions. Still, these scanning electron micrographs did suggest that these spherulites were space-filling, and this indicates that the interspherulitic segregation was minimal.

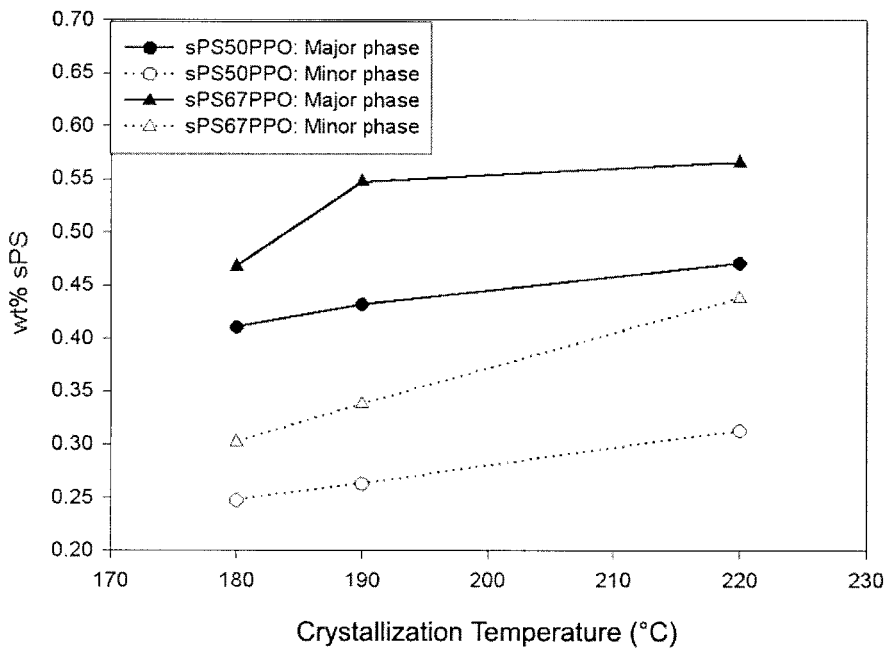

Figure 6 Variations in the amorphous phase compositions for cold-crystallized blends, as calculated from DMA transition temperatures and the Gordon–Taylor relation.

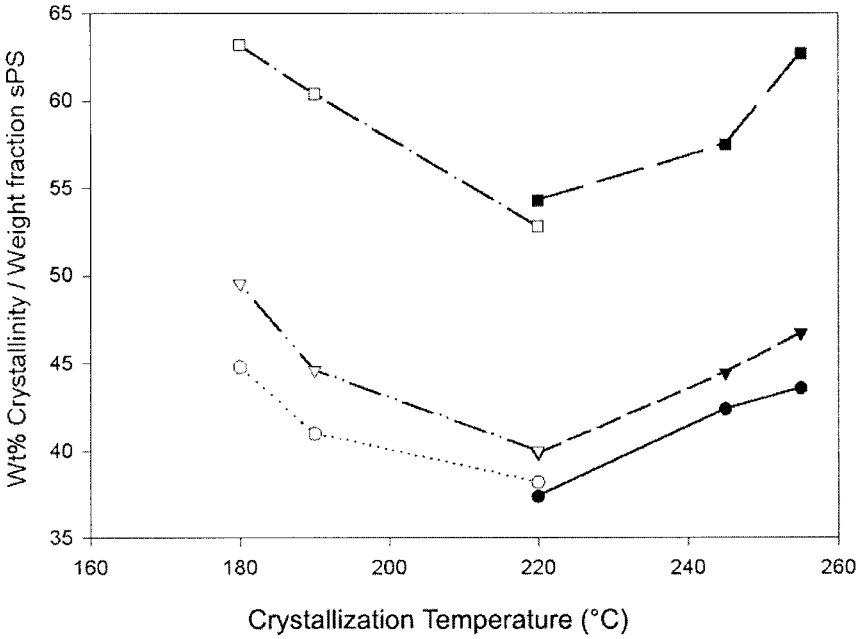

Figure 7 WAXD crystallinity of cold- and melt-crystallized sPS/PPO blends on the basis of the sPS content. Circles represent sPS50PPO blends, triangles represent sPS67PPO, and squares represent neat sPS. Open data points represent cold-crystallized samples, and closed data points represent melt-crystallized samples.

Melt-crystallized blends

The tan δ scans for melt-crystallized sPS/PPO blends were qualitatively similar to those of the cold-crystallized blends. The variation in tan δ for the melt-crystallized sPS50PPO blends is shown in Figure 8. All scans showed a primary composition-dependent relaxation peak. As for the cold-crystallized blends, melt-crystallized blends also showed distinct shoulders (or separate peaks) to the primary relaxation peak. These shoulders were more prominent in the blends crystallized at higher temperatures, which correspond to lower supercoolings and lower crystallization rates. Slower crystallization (at higher temperatures) reduced the transition temperature of the pri-

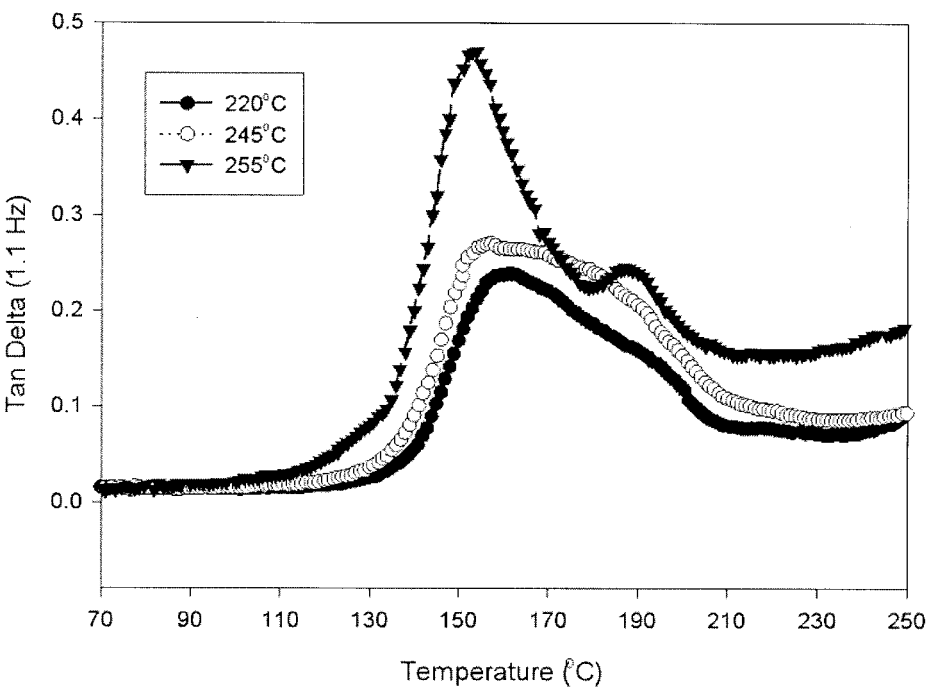

Figure 8 DMA tan δ values of melt-crystallized sPS50PPO blends.

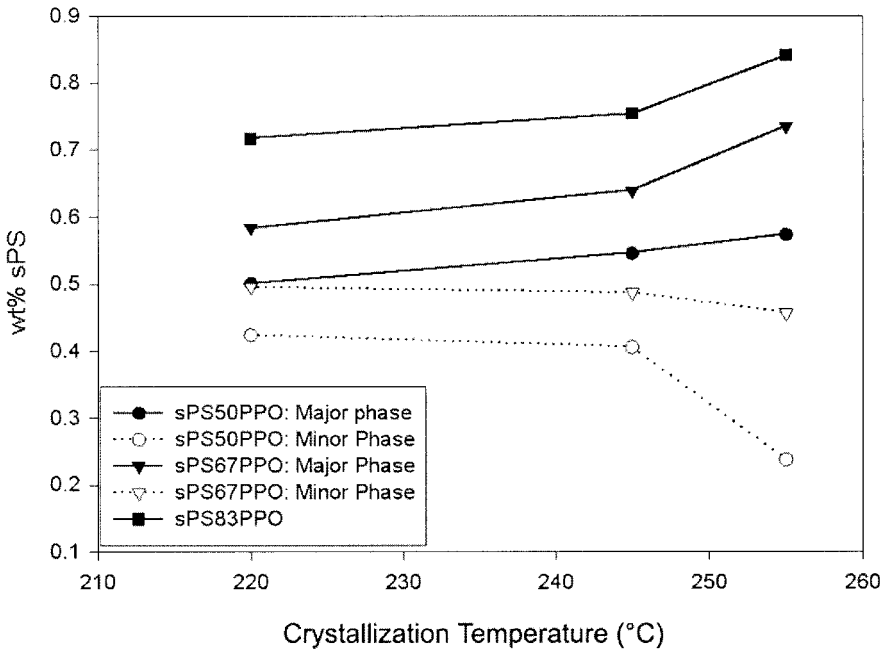

Figure 9 Variations in the amorphous phase compositions for melt-crystallized blends, as calculated from DMA transition temperatures and the Gordon–Taylor relation.

mary relaxation and increased the temperature of the weaker relaxation.

The shoulder (or second peak) in the DMA scans of the melt-crystallized blends was most visible in the sPS50PPO blend crystallized at 255°C. The corresponding E' decreased continuously with temperature, and there was no evidence of recovery due to crystallization. These data suggest that the two well-defined relaxation peaks were due to the segregation of the initially homogeneous melt into two different amorphous phases, which consisted of both polymers but with different compositions. An increase in the PPO content increased T_g and pushed the relaxations to higher temperatures. For a fixed composition (Fig. 8), an increase in T_c increased the difference between the temperatures of the major and minor relaxations. This suggests that slower crystallization facilitated the formation of phases of increasingly different compositions. Faster crystallization (at lower temperatures) resulted in much broader, overlapping relaxation peaks. This is an indication that the segregation of PPO between two distinct amorphous populations was less well defined in these samples.

The decreasing temperatures of the primary relaxation suggest an increase in the sPS (lower T_g component) content in the major phase at the cost of the second minor phase. This observation is in contrast to the composition behavior of the amorphous phases in cold-crystallized blends, in which both phases became depleted of sPS with slower crystallization at lower temperatures. This observation seems realistic in view of the lesser constraints on the diffusion of the low-T_g amorphous component in the melt with fewer nuclei than the cold-crystallized blend.

As shown in Figure 9, for both sPS50PPO and sPS67PPO blends, the concentrations of the major and minor phases diverged away from each other with increasing T_c. Although the major phase became sPS-rich, the minor phase was depleted of sPS and became PPO-rich. Therefore, it can be concluded that slower crystallization at a higher temperature increased the degree of segregation in the melt-crystallized blends.

The decrease in sPS in the minor amorphous phase with increasing T_c also corresponded to an increasing relative crystallinity. The growing sPS crystal front absorbed sPS and rejected PPO. As a result, the sPS concentration was smallest near the growing crystal front. The concentration of the PPO changed in the reverse manner. It was highest near the growth front and decreased with increasing distances. A schematic diagram of the growing lamellar fronts in a bundle and the corresponding interlamellar and interfibrillar regions is shown in Figure 10. The crystals act as sources of PPO and sinks of sPS. Because of the proximity of the interlamellar regions to the crystal growth front, they should have the lowest sPS content and, therefore, the highest relaxation temperatures. Because the interspherulitic segregation of the amorphous material was not observed, the interfibrillar region should then form the major sinks of the amorphous sPS and noncrystallizable PPO. These regions should have high amorphous sPS and low PPO concentrations and, therefore, lower relaxation temperatures. Consequently, it can be concluded that the high-

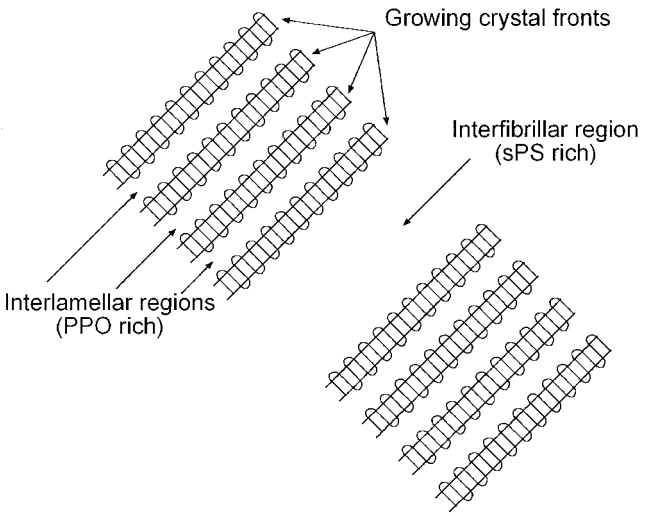

Figure 10 Schematic diagram of interlamellar and interfibrillar amorphous regions and their expected compositions.

intensity peak at lower temperatures was due to the relaxation of the amorphous material present in the interfibrillar regions. The smaller intensity shoulder observed at higher temperatures was due to the relaxation of amorphous interlamellar regions.

CONCLUSIONS

The sPS/PPO blend formed a completely miscible system in the melt state. The phase separation that did occur was induced by the crystallization of sPS. In most cases, two amorphous phases were formed. The composition of the major amorphous phase (by mass fraction) was close to the initial blend composition. In the melt-crystallized blends, the major phase consisted of sPS-rich interfibrillar regions and PPO-rich interlamellar regions. In cold-crystallized blends, although the sPS concentration in both phases decreased with slow crystallization at lower supercoolings, the scale of segregation of PPO was much lower.

The authors thank Dow Chemical Co. for kindly providing sPS.

References

1. Guerra, G.; Vitagliano, V. M.; Rosa, C. D.; Petraccone, V.; Corradini, P.; Karasz, F. Polym Commun 1991, 32, 30.
2. Wu, F. S. Master's Thesis, National Cheng Kung University, 1997.
3. Cimmino, S.; Di Pace, E.; Martucelli, E.; Silvestre, C. Polymer 1993, 34, 2799.
4. Kit, K. M.; Schultz, J. M. J Polym Sci Part B: Polym Phys 1998, 36, 873.
5. Khambatta, F. B.; Russell, T.; Warner, F.; Stein, R. S. J Polym Sci Polym Phys Ed 1976, 14, 1391.
6. Wenig, W.; Karasz, F. E.; MacKnight, W. J.; Stein, R. S. J Appl Phys 1975, 46, 4194.
7. Hahn, B.; Hermann-Schonherr, O.; Wendroff, J. Polymer 1987, 28, 201.
8. Russell, T. P.; Ito, H.; Wignall, G. D. Macromolecules 1988, 21, 1703.
9. Hsiao, B. S.; Sauer, B. B. J Polym Sci Part B: Polym Phys 1993, 31, 901.
10. Keith, H. D.; Padden, F. J. J Appl Phys 1964, 35, 1286.
11. Hudson, S. D.; Davis, D. D.; Lovinger, A. J. Macromolecules 1992, 25, 1759.
12. Harris, J. E.; Robeson, L. M. Contemporary Topics in Polymer Science; Plenum: New York, 1989; Vol. 6.
13. Bristow, J. F.; Kalika, D. S. Macromolecules 1994, 27, 1808.
14. Krishnaswamy, R. J.; Kalika, D. S. Polym Eng Sci 1996, 36, 786.
15. Kelly, F. N.; Bueche, F. J Polym Sci 1961, 50, 549.
16. Fox, T. G. Bull Am Phys Soc 1956, 2, 123.
17. Gordon, M.; Taylor, J. S. J Appl Chem 1952, 2, 493.
18. Couchman, P. R.; Karasz, F. E. Macromolecules 1978, 11, 117.
19. Aubin, M.; Prud'homme, R. E. Polym Eng Sci 1988, 28, 1355.